On the Atmospheric Responses to Tropical Pacific Heating during the Mature Phase of El Niño

CHUNZAI WANG

NOAA/Atlantic Oceanographic and Meteorological Laboratory, University of Miami, Miami, Florida

(Manuscript received 19 March 1999, in final form 16 December 1999)

ABSTRACT

The atmospheric heating and sea surface temperature (SST) anomalies during the mature phase of El Niño are observed to show both eastern and western Pacific anomaly patterns, with positive anomalies in the equatorial eastern/central Pacific and negative anomalies in the off-equatorial western Pacific. The detailed spatial patterns of the heating anomalies differ from the SST anomalies. The heating anomalies are more equatorially confined than the SST anomalies, and maxima of positive and negative heating anomalies are located farther to the west than the SST anomalies. The Gill–Zebiak atmospheric model assumes that the atmospheric initial heating has the same spatial patterns as the SST anomalies. This assumption results in some unrealistic model simulations for El Niño.

When the model heating anomaly forcing is modified to resemble the observed heating anomalies during the mature phase of El Niño, the model simulations have been improved to 1) successfully simulate equatorial easterly wind anomalies in the western Pacific, 2) correctly simulate the position of maximum westerly wind anomalies, and 3) reduce unrealistic easterly wind anomalies in the off-equatorial eastern Pacific. This paper shows that off-equatorial western Pacific negative atmospheric heating (or cold SST) anomalies are important in producing equatorial easterly wind anomalies in the western Pacific. These off-equatorial cold SST anomalies in the western Pacific also contribute to equatorial westerly wind anomalies observed in the central Pacific during the mature phase of El Niño. Although off-equatorial cold SST anomalies in the western Pacific are smaller than equatorial positive SST anomalies in the eastern Pacific, they are enough to produce atmospheric responses of comparable magnitude to the equatorial eastern Pacific. This is because the atmospheric mean state is convergent in the western Pacific and divergent in the equatorial eastern Pacific. By either removing the atmospheric mean convergence or removing off-equatorial cold SST anomalies in the western Pacific, the atmospheric responses show no equatorial easterly wind anomalies in the western Pacific. In the Gill–Zebiak model, the mean wind divergence field is an important background state, whereas the mean SST is secondary.

1. Introduction

Since Bjerknes (1966, 1969) visualized a close relation between the Walker circulation and east–west sea surface temperature (SST) contrast in the equatorial Pacific Ocean, the El Niño–Southern Oscillation (ENSO) has been recognized as a phenomenon involving the ocean–atmosphere interactions and has been intensively studied (e.g., Philander 1990; McCreary and Anderson 1991; Neelin et al. 1998). A comprehensive description of a composite El Niño was given by Rasmusson and Carpenter (1982), using observed surface wind and SST data from 1949 to 1976. This observational study clearly described the evolution of El Niño and its spatial structures for six warm episodes from 1949 to 1976. They also noted that El Niño is phase-locked to the seasonal cycle. In the far eastern Pacific, El Niño begins around Christmastime and peaks in the boreal late spring of the El Niño year. In the equatorial eastern/central Pacific, positive SST anomalies occur in the boreal spring and peak near the end of the El Niño year. Many other observational studies have also described the evolution of ENSO (e.g., Rasmusson and Wallace 1983; Deser and Wallace 1990; Nigam and Shen 1993; Mitchell and Wallace 1996). Most of these studies focused on and emphasized ENSO eastern/central Pacific patterns although western Pacific interannual variability appeared in these studies, in all probability because interannual anomalies in the eastern/central Pacific are larger than those in the western Pacific.

By emphasizing ENSO western Pacific anomaly patterns, Wang et al. (1999b) obtained composite horizontal structure patterns for peak El Niño and La Niña using the Comprehensive Ocean–Atmosphere Data Set (COADS) data (Woodruff et al. 1987) from January 1950 to December 1992 and outgoing longwave radi-

Corresponding author address: Dr. Chunzai Wang, Physical Oceanography Division, NOAA/Atlantic Oceanographic and Meteorological Laboratory, 4301 Rickenbacker Causeway, Miami, FL 33149.
E-mail: wang@aoml.noaa.gov

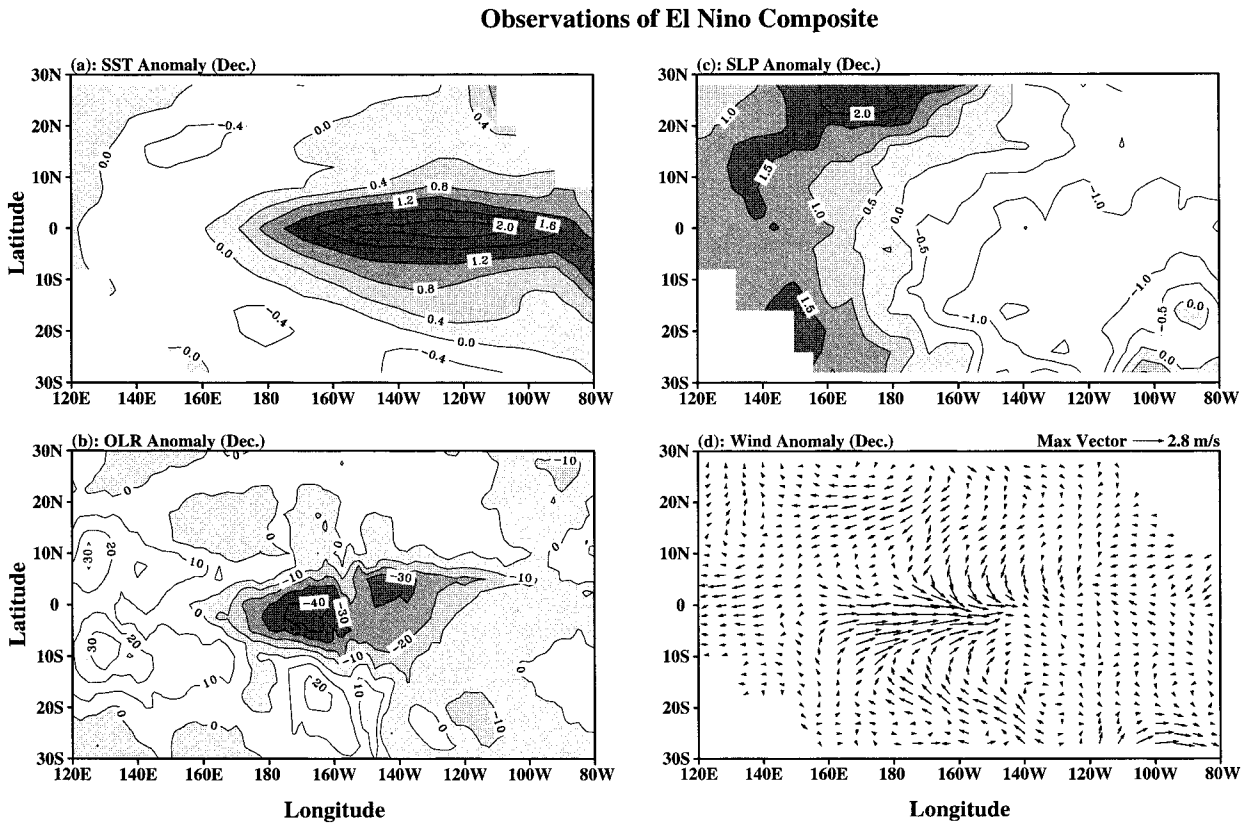

FIG. 1. The peak El Niño composite of (a) SST anomalies (°C), (b) OLR anomalies (W m^{-2}), (c) SLP anomalies (mb), and (d) surface wind anomolies (m s^{-1}). The composite is formed by taking the average Dec anomaly for 1957, 1965, 1972, 1982, 1986, and 1991 (Wang et al. 1999b). The data are based on COADS data from Jan 1950 to Dec 1992 and OLR data from Jan 1974 to Dec 1992.

ation (OLR) data from January 1974 to December 1992. The peak El Niño composite, shown in Fig. 1, was calculated by taking the average December anomaly of the El Niño years from 1950 to 1992. For the peak of the El Niño composite, when maximum warm SST anomalies occur in the equatorial eastern Pacific, maximum cold SST anomalies are located to the north and south of the equator in the western Pacific rather than on the equator. Since the atmospheric convection over the western Pacific warm pool shifts to the equatorial central Pacific during the warm phase of ENSO, the region of low OLR anomalies is located to the west of equatorial eastern Pacific maximum warm SST anomalies. Similar to the relative position of the SST and OLR anomalies in the equatorial eastern and central Pacific, the off-equatorial region of high OLR anomalies is positioned west of the off-equatorial region of cold SST anomalies in the western Pacific. The off-equatorial western Pacific cold SST anomalies are also accompanied by off-equatorial western Pacific high SLP anomalies. As shown in Fig. 1, the off-equatorial high SLP anomalies generate equatorially convergent wind anomalies that turn anticyclonically to equatorial easterly wind anomalies over the far western Pacific. The nearly out-of-phase behavior between the eastern and western tropical Pacific is also observed during the cold phase of ENSO, but with anomalies of opposite sign. The 1997–98 El Niño is no exception, also showing the western Pacific patterns (Wang and Weisberg 2000). The western Pacific patterns were also present in other studies (e.g., Rasmusson and Carpenter 1982; Rasmusson and Wallace 1983; Graham and White 1988, 1991; White et al. 1987, 1989; Kessler 1990; Chao and Philander 1993; Nigam and Shen 1993; Mestas-Nunez and Enfield 2000) but were more or less ignored and their potential importance was not emphasized.

Using the linear momentum equations and surface winds derived from the Florida State University Pacific pseudostress fields, Zebiak (1990) estimated surface pressure and then obtained the adjusted winds. The adjusted winds and pressure are used to infer atmospheric forcing within the context of a dynamical model. The inferred atmospheric forcing along with the observed anomalies of OLR (with the sign reversed), highly reflective cloud (HRC), and SST for December 1982 are shown in Fig. 2. All of these fields show both eastern and western Pacific anomaly patterns, with positive anomalies in the equatorial central/eastern Pacific and negative anomalies in the off-equatorial western Pacific. However, the detailed spatial patterns between the SST

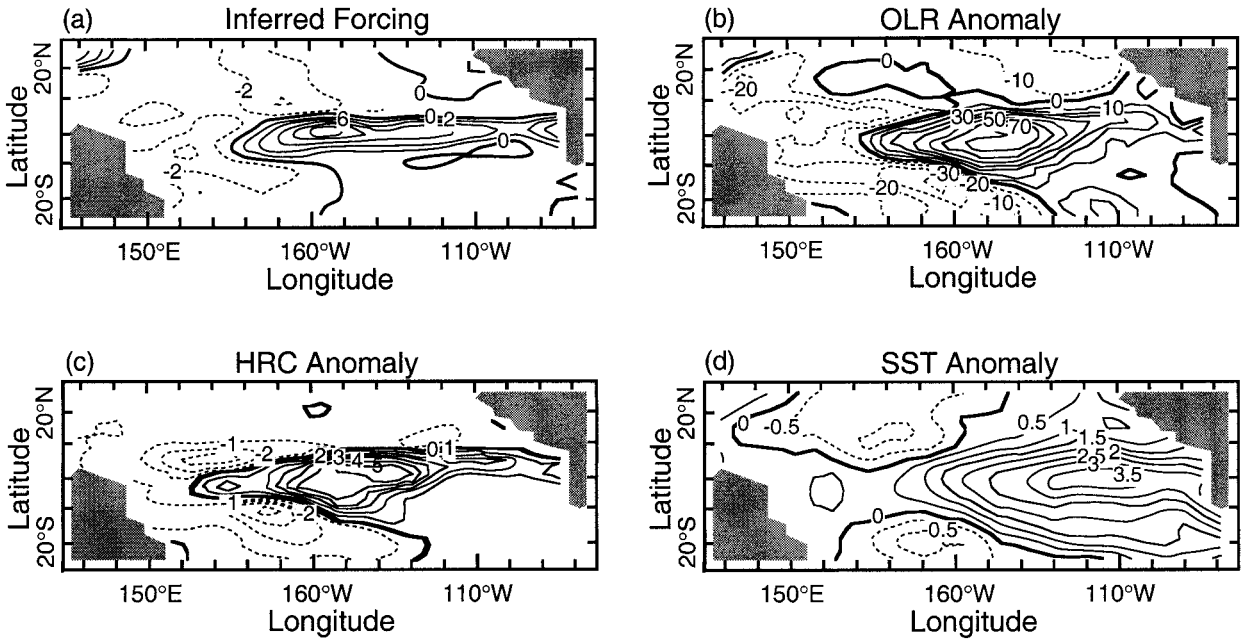

FIG. 2. (a) Inferred atmospheric heating forcing, (b) OLR, (c) HRC, and (d) SST anomalies for Dec 1982 (Zebiak 1990). OLR anomalies are in W m^{-2} with the sign reversed. HRC anomalies are units of days per month with significant HRC present. SST anomalies are in °C.

anomalies and the anomaly fields manifesting the atmospheric heating differ (also see Fig. 1). First, the inferred atmospheric forcing, OLR, and HRC anomalies are tightly confined to the equator, whereas the SST anomalies show a broad meridional scale with the SST anomalies extending into the subtropics. Second, maxima of the inferred atmospheric forcing, OLR, and HRC anomalies are located to the west of the maximum SST anomalies, consistent with Fig. 1.

Many numerical models, from simple atmospheric models to complex atmospheric general circulation models, have been developed to study atmospheric responses to heating forcing (e.g., Gill 1980; Zebiak 1986; Lindzen and Nigam 1987; Kleeman 1991; Battisti et al. 1999; Seager and Zebiak 1995; Wang and Li 1993; Latif et al. 1990). The Zebiak (1986) version of the Gill (1980) atmosphere (hereafter, the Gill–Zebiak model) is the first simple atmospheric model obtaining ENSO simulations that are comparable to more complex atmospheric models. This model has significantly improved the results of Zebiak's (1982) model in which the atmospheric heating is assumed to be linearly proportional to SST anomalies, by considering an additional heating source associated with the low-level moisture convergence feedback process. In particular, the feedback process results in a reduction of scale in the atmospheric anomalous divergence field and an increase in amplitude of the atmospheric responses. Despite the improvement, the model still has difficulty in reproducing some of the observational features as commented on by Zebiak (1986), Zebiak and Cane (1987), and Wang et al. (1999b). First, the model cannot simulate equatorial easterly wind anomalies adequately in the western Pacific during the mature phase of El Niño. Second, the model's maximum equatorial westerly wind anomalies are located farther to the east than those in the observations. Third, the model produces unrealistic easterly wind anomalies in the off-equatorial eastern Pacific.

These discrepancies may be due to the assumption of the same spatial patterns between the atmospheric initial heating and SST anomalies in the model, in additional to owing to the simple physics of the Gill–Zebiak model. As observed in Figs. 1 and 2, the spatial patterns of the atmospheric heating are different from those of the SST anomalies. The model assumes that atmospheric initial heating anomalies are linearly proportional to SST anomalies, and thus heating anomalies have the same horizontal structure as the SST anomalies. Recently, Battisti et al. (1999) summarized all of the simple atmospheric models and highlighted some inconsistencies between model derivation and the values of several of the parameters. In their paper, they did not consider and study the causal relationships between heating and model simulations. The present paper investigates how the spatial pattern differences between the heating and SST anomalies in the Gill–Zebiak model affect model simulations. This paper identifies which of the mean background states in the Gill–Zebiak model is important and shows why it is important. Observations in Fig. 1a show that negative SST anomalies in the off-equatorial western Pacific are smaller than positive SST anomalies in the equatorial eastern Pacific. It will be shown that these smaller off-equatorial negative SST anomalies are sufficient to produce equatorial easterly wind anomalies in

the western Pacific during the mature phase of El Niño. If the off-equatorial negative SST anomalies in the western Pacific are removed, the model shows no equatorial easterly wind anomalies produced in the western Pacific and a decrease in westerly wind responses in the equatorial central Pacific. This paper also examines the seasonal dependence of atmospheric responses and discusses its possible impact on the ENSO phase-locking to the seasonal cycle. The rest of the paper is organized as follows. Section 2 briefly introduces the Gill–Zebiak model used in this paper, and section 3 presents the main results. A summary and discussion are given in section 4.

2. The model

Gill (1980) developed a steady-state, linear, equatorial β-plane, reduced-gravity model to elucidate basic features of tropical atmospheric responses to diabatic heating anomaly, Q. Zebiak (1986) considered Q to contain two parts: the atmospheric initial heating and the low-level moisture convergence feedback. The atmospheric initial heating, Q_T, is expressed as

$$Q_T = \alpha T \exp[(\overline{T} - 29.8)/16.7], \quad (1)$$

where the constant $\alpha = 0.031$ m^2 s^{-3} °C^{-1}. The Q_T depends upon SST anomaly, T, and mean SST, $\overline{T}$. A larger $\overline{T}$ will result in more heating, Q_T, for the same T. Thus, the western Pacific will give relatively more atmospheric initial heating than the eastern Pacific for equal SST anomalies since the mean state in the western Pacific Ocean is much warmer than the eastern Pacific Ocean. The low-level moisture convergence feedback is parameterized in terms of both the mean wind divergence, $\overline{C}$, and the anomalous wind divergence, C:

$$Q_C = \begin{cases} 0, & \text{if } (\overline{C} + C) > 0, \quad \overline{C} > 0 \quad (2a) \\ -\beta C, & \text{if } (\overline{C} + C) \le 0, \quad \overline{C} \le 0 \quad (2b) \\ -\beta(\overline{C} + C), & \text{if } (\overline{C} + C) \le 0, \quad \overline{C} > 0 \quad (2c) \\ \beta\overline{C}, & \text{if } (\overline{C} + C) > 0, \quad \overline{C} \le 0, \quad (2d) \end{cases}$$

where the efficiency factor for the convergence feedback process $\beta = 1.6 \times 10^4$ m^2 s^{-2} (Zebiak 1986; Zebiak and Cane 1987). Here Q_C is incorporated into the model using an iterative procedure in which the heating at each iteration depends on the convergence field from the previous iteration. The model is initially forced by Q_T to produce C that is used to calculate Q_C [$\overline{C}$ is specified based on observations of Rasmusson and Carpenter (1982)]. Then the total atmospheric heating $Q = Q_T + Q_C$ is used to force the atmosphere for the next step. The solution is calculated iteratively until a near steady state is reached (see Zebiak 1985).

Zebiak (1986) has shown that the model with the low-level moisture convergence feedback improves the ability of model simulations by amplifying magnitudes of atmospheric responses and by decreasing the meridional scale of the model divergence anomaly field. As Zebiak (1986) pointed out, the moisture convergence feedback in his model differs from that of Webster (1981) by including the influence of the mean wind divergence field. A heating anomaly should be expected to grow only if the total wind field is convergent since only then can there be an anomalous influx of moisture. If the mean wind field is ignored, the result is that positive heating anomalies are always enhanced and negative heating anomalies are never enhanced. It will be shown in the next section that the mean wind divergence field associated the western Pacific warm pool convection is important for correctly simulating wind anomalies in the western and central Pacific.

The weakness of Eq. (1) is that the atmospheric initial heating anomalies are linearly proportional to SST anomalies. That is, spatial patterns of SST anomalies determine spatial patterns of the atmospheric heating. However, as evidenced in Figs. 1 and 2, the horizontal spatial patterns of the atmospheric heating are observed to differ from those of the SST anomalies. First, the atmospheric heating is tightly confined to the equator, whereas the SST anomalies have a broader meridional structure. Second, maxima of positive and negative heating anomalies are located farther west than those of SST anomalies. These differences suggest that the atmospheric heating of Eq. (1) should be modified to

$$Q_T = \alpha A(T) \exp[(\overline{T} - 29.8)/16.7]. \quad (3)$$

Function $A(T)$ represents spatial relationships between the atmospheric heating and SST anomalies.

3. Atmospheric responses to heating

In this section, we perform many experiments to explore features of atmospheric responses to tropical Pacific heating using the Gill–Zebiak model. In all calculations, the mean SST and the mean wind divergence are specified from the December climatologies since we are interested in atmospheric responses during the mature phase of El Niño, except for experiments that study seasonal dependence of atmospheric responses.

a. The same structure between atmospheric initial heating and SST anomalies

The Gill–Zebiak model associated with the standard heating formulation is first used to show how the atmosphere responds to tropical Pacific SST anomalies. The SST anomalies are taken from the observed El Niño composite of Fig. 1a. The initial heating, Q_T, is calculated based on the standard formulation of Eq. (1). The resulting Q_T is shown in Fig. 3a. According to this formulation, the horizontal structure of the initial heating remains the same pattern as the SST anomalies since they are assumed to be linearly related. Since the initial heating also depends upon $\overline{T}$, which has larger values in the western Pacific than in the eastern Pacific, enhancement in the initial heating is relatively large in the western Pacific. This Q_T is used to force the model,

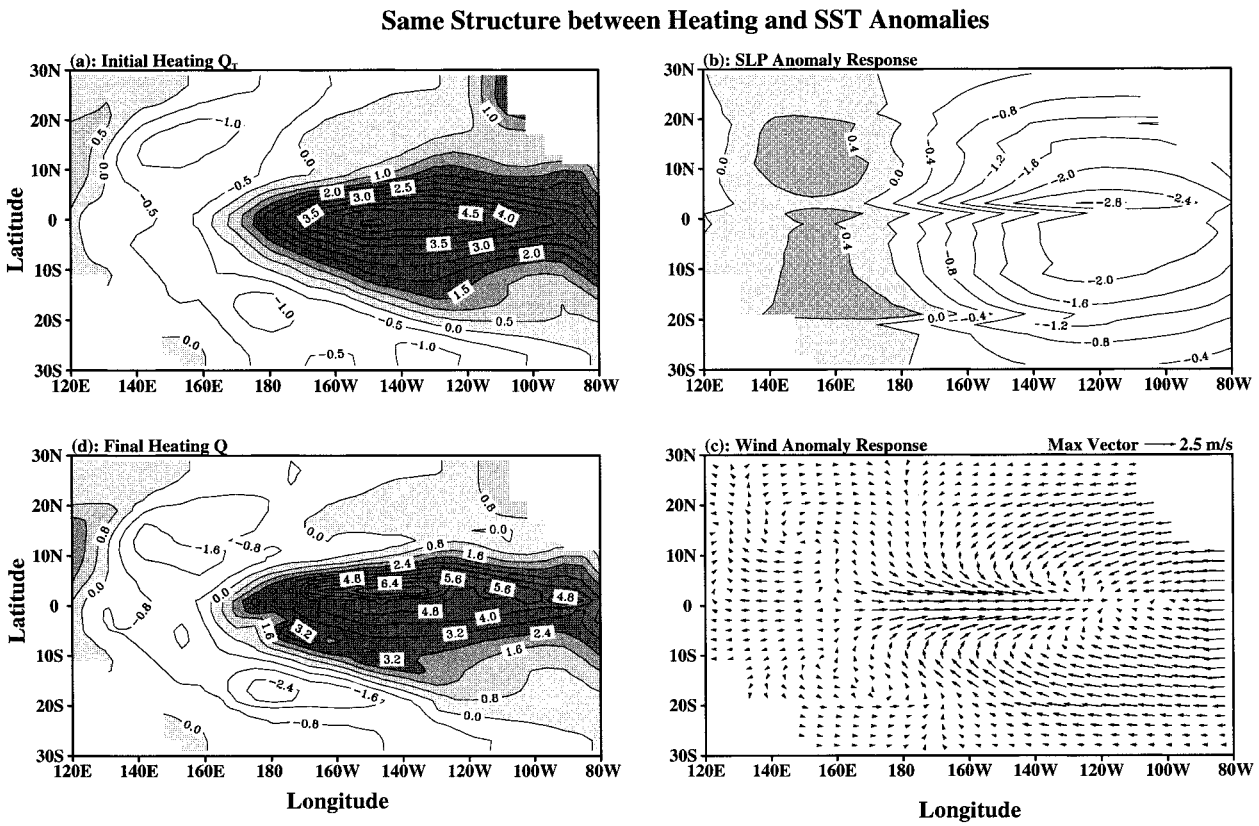

FIG. 3. Atmospheric responses to initial heating anomalies that has the same spatial structure as the SST anomalies. (a) Atmospheric initial heating Q_T (10^{-2} m^2 s^{-3}), (b) SLP anomaly response (mb), (c) surface wind anomaly response (m s^{-1}), and (d) atmospheric final total heating $Q = Q_T + Q_C$ (10^{-2} m^2 s^{-3}).

resulting in the sea level pressure (SLP) anomalies, surface wind anomalies, and final atmospheric total heating anomalies ($Q = Q_T + Q_C$) shown in Figs. 3b, 3c, and 3d, respectively. Associated with positive heating anomalies in the equatorial eastern Pacific and negative heating anomalies in the off-equatorial western Pacific, the atmospheric SLP responses consist of low SLP anomalies in the equatorial eastern Pacific and high SLP anomalies in the off-equatorial western Pacific. Due to this SLP distribution, equatorial westerly wind anomalies are produced in the central Pacific and weak equatorial easterly wind anomalies are induced in the western Pacific.

Comparison with observations in Fig. 1 shows that the model captures the basic features of tropical Pacific SLP and surface wind anomalies. However, there are many differences between observations and the model simulations. First, the magnitudes of both equatorial easterly wind anomalies and off-equatorial SLP anomalies in the western Pacific are smaller than those of observations. Second, the position of the maximum model westerly wind anomalies is farther east than observations. Third, the model produces unrealistic off-equatorial easterly wind anomalies in the eastern Pacific. The reason for these differences may be attributed to heating spatial pattern differences between observations and the model. The observed heating anomalies are more equatorially confined than the model heating anomalies. Maxima of the observed positive and negative heating anomalies extend farther west than those in the model. Although the model total heating anomalies are improved, they still differ from the observed anomaly fields manifesting the atmospheric heating (see Figs. 3d, 1, and 2). In the next section, we will investigate how the horizontal structure of atmospheric heating affects the model simulations.

b. Modified heating

To see whether or not the model discrepancies are due to the assumption that the atmospheric initial heating anomalies have the same spatial structure as the SST anomalies, we modify the atmospheric initial heating according to Eq. (3). For the purpose of obtaining a similar heating structure to observations in Figs. 1 and 2, we construct the spatial function of $A(T)$ by the following two steps. First, the negative off-equatorial SST anomalies are shifted westward and equatorward. Second, the positive equatorial SST anomalies are projected on an elliptical function:

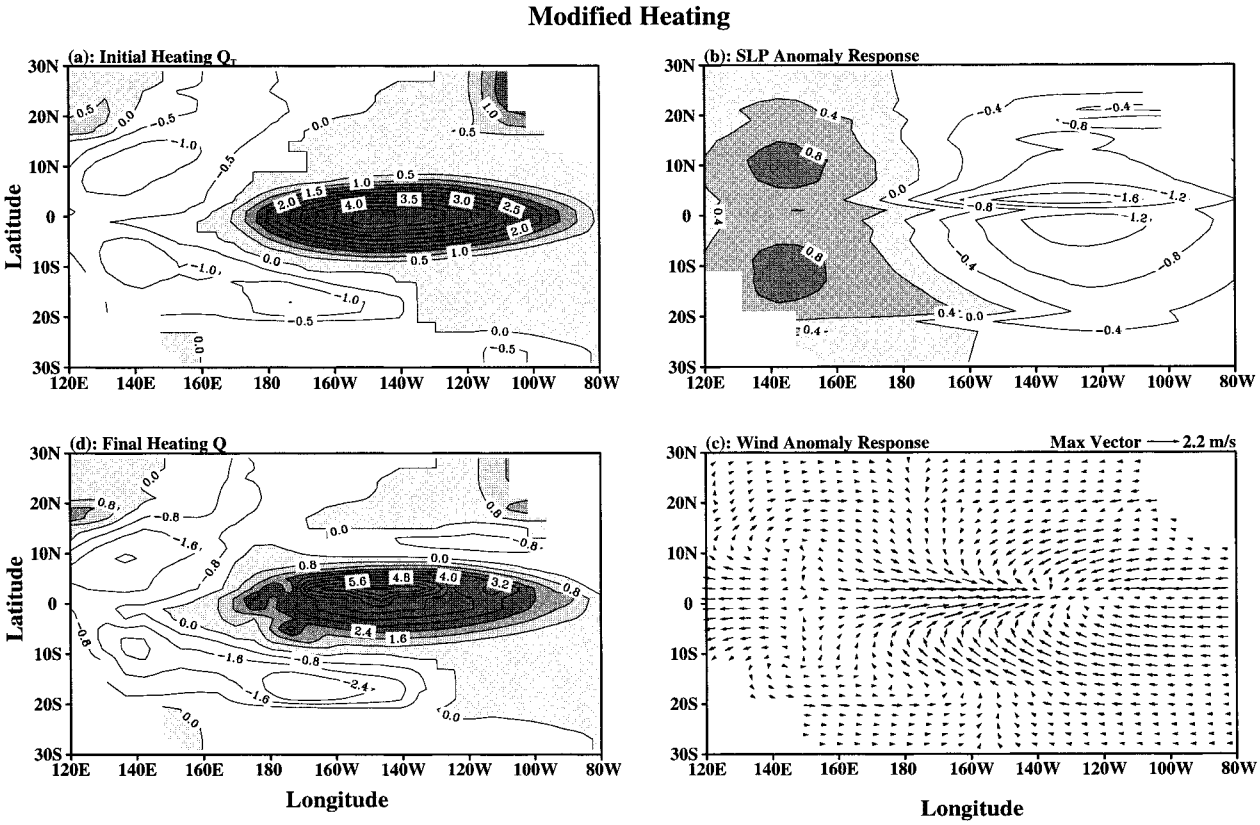

FIG. 4. Atmospheric responses to modified initial heating anomalies. (a) Atmospheric initial heating Q_T (10^{-2} m^2 s^{-3}), (b) SLP anomaly response (mb), (c) surface wind anomaly response (m s^{-1}), and (d) atmospheric final total heating $Q = Q_T + Q_C$ (10^{-2} m^2 s^{-3}).

$$\frac{(x - x_0)^2}{a^2} + \frac{y^2}{b^2} = 1, \tag{4}$$

where $x_0 = 151.875°$W, $a = 80°$, and $b = 10°$. The resulting atmospheric initial heating is shown in Fig. 4a. The modified initial heating is closer to observed anomaly fields manifesting atmospheric heating than the unmodified case of Fig. 3a. Both positive and negative heating anomalies are more confined to the equator, and maxima of these positive and negative heating anomalies extend farther to the west.

With this initial heating, the atmospheric responses (wind and SLP) show a decrease in magnitude over the eastern Pacific and an increase in magnitude over the western Pacific. In particular, the magnitude of off-equatorial high SLP anomalies in the western Pacific is doubled. Associated with the increase in off-equatorial high SLP anomalies in the western Pacific, equatorial easterly wind anomalies in the western Pacific are increased to observed values. The maximum of the equatorial westerly wind anomalies extends farther west than the unmodified case of Fig. 3c. Comparison between Figs. 3c and 4c shows that some of the unrealistic off-equatorial easterly wind anomalies in the eastern Pacific for the unmodified case have been somewhat reduced. Associated with the modified initial heating, the model final total heating of Fig. 4d also shows a closer structure to the observed heating forcing.

Why does the modified heating produce relatively realistic atmospheric responses? Gill (1980) showed that the atmospheric responses to a heating consist of atmospheric Kelvin and Rossby waves with an equatorial Rossby radius of deformation of about 10°. In the central and eastern Pacific, when the positive heating anomalies in the modified case are projected onto Hermite functions, the projections will be weaker than the unmodified case since the meridional scale of positive heating anomalies for the modified case is more equatorially confined. Therefore, the magnitude of the atmospheric responses in the central and eastern Pacific is reduced, and unrealistic off-equatorial easterly wind anomalies in the eastern Pacific are also reduced. In the western Pacific, the modified heating field shifts the off-equatorial maximum negative heating anomalies equatorward to about 10°N and 10°S. This shift makes the projection of atmospheric Rossby waves stronger (recall that the atmosphere has an equatorial Rossby radius of deformation of about 10°). The model atmospheric responses in the western Pacific thus become stronger.

Magnitudes of off-equatorial negative heating anomalies (or SST anomalies) in the western Pacific are

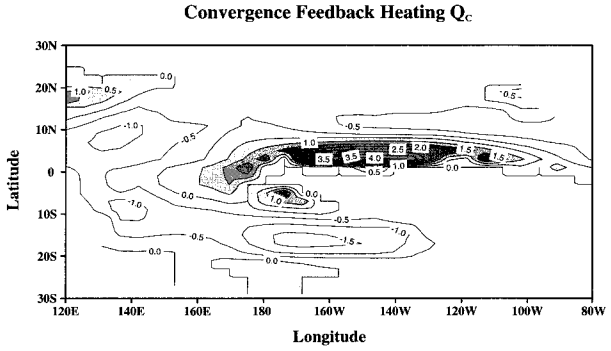

FIG. 5. The heating anomalies of the low-level moisture convergence feedback Q_C for the experiment shown in Fig. 4.

smaller than those of equatorial positive heating anomalies (or SST anomalies) in the eastern Pacific. Why can these small off-equatorial anomalies in the western Pacific produce atmospheric responses of comparable amplitude to those in the equatorial eastern Pacific? This is attributed to the model low-level moisture convergence feedback, Q_C, that depends on the mean wind divergence field. In the western Pacific, the mean wind field in December is convergent (shown later in Fig. 10d) and the magnitude of this mean convergence is large compared with the anomalous divergence. The anomalous convergence feedback case of Eq. (2b) applies, with $Q_C = -\beta C$, and the western Pacific thus shows off-equatorial negative heating anomalies of Q_C as shown in Fig. 5. In the eastern Pacific, there is a meridional asymmetry of mean states. The mean wind convergence is located to the north of the equator, associated with the intertropical convergence zone (ITCZ), whereas the mean wind fields are divergent to the south of the ITCZ. In the region south of the equator and near the equator, where the strength of the mean divergence is large compared with anomalous convergence, the no-feedback case of Eq. (2a) applies with $Q_C = 0$. This region thus shows no low-level moisture convergence feedback as shown in Fig. 5. The distribution of Q_C causes an increase of total heating anomalies in the off-equatorial western Pacific, but no gain in the equatorial eastern Pacific. The mean atmospheric convergent state associated with the western Pacific warm pool convection enhances heating anomalies in the western Pacific. Therefore, smaller off-equatorial cold SST anomalies in the western Pacific produce atmospheric responses of comparable amplitude to those in the equatorial eastern Pacific.

c. *Effects of mean background states*

There are two mean background states in the Gill–Zebiak model that are specified as monthly climatologies. One is the atmospheric mean wind divergence field and the other is the oceanic mean SST field. Effects of these mean states on tropical atmospheric responses can be assessed by comparing experiments with and without these mean background states. Figure 6 shows the model atmospheric responses without the mean wind divergence field. Comparison with Fig. 4 shows that the mean wind divergence field plays an important role in atmospheric responses. SLP and wind anomaly responses in the eastern Pacific are larger than the experiment with the mean wind divergence, whereas in the western Pacific they are smaller than the experiment with the mean wind divergence. In particular, associated with the smaller western Pacific off-equatorial high SLP anomalies, equatorial easterly wind anomalies in the western Pacific are very weak (nearly zero). According to the convergence feedback of Eq. (2), if the mean wind divergence is zero, Q_C only depends upon anomalous wind divergence. The negative initial heating anomalies in the off-equatorial western Pacific result in anomalous divergence ($C > 0$), whereas the positive initial heating anomalies in the equatorial eastern Pacific induce anomalous convergence ($C < 0$). Equation (2) shows that Q_C in the western Pacific and in the eastern Pacific are zero and $-\beta C$, respectively. Thus, Q_C enhances the total heating anomalies in the equatorial eastern Pacific, but it does not contribute to the heating anomalies in the western Pacific for the experiment without the mean divergence (see Figs. 6a,d). In comparison with the experiment with the mean divergence, the final total heating anomalies in the eastern Pacific and in the western Pacific are increased and decreased, respectively. Without the mean divergence field, the smaller off-equatorial western Pacific heating anomalies are not enough to produce equatorial easterly wind anomalies in the western Pacific. Comparison between Figs. 4 and 6 also shows that SLP responses in the eastern Pacific for the experiment without the mean wind divergence are more symmetric about the equator (if the mean SST field is also removed, the atmospheric responses will be exactly symmetric), suggesting that the mean wind divergence field also plays an important role in asymmetric responses in the eastern Pacific.

An experiment with a constant mean SST ($\overline{T} = 27.0°C$) was also performed, as shown in Fig. 7. The experiment shows similar responses to Fig. 4. In particular, SLP and wind anomalies in the central and eastern Pacific are similar to those in Fig. 4. Although off-equatorial high SLP anomalies in the western Pacific are reduced a little bit (compared with Fig. 4), the off-equatorial western Pacific anomaly patterns are enough to produce strong equatorial easterly wind anomalies in the western Pacific. This suggests that spatial distribution of the mean SST background state in the Gill–Zebiak model plays a secondary role in atmospheric responses.

d. *Role of off-equatorial western Pacific anomaly patterns*

The role of off-equatorial western Pacific anomaly patterns in model responses can be addressed by running

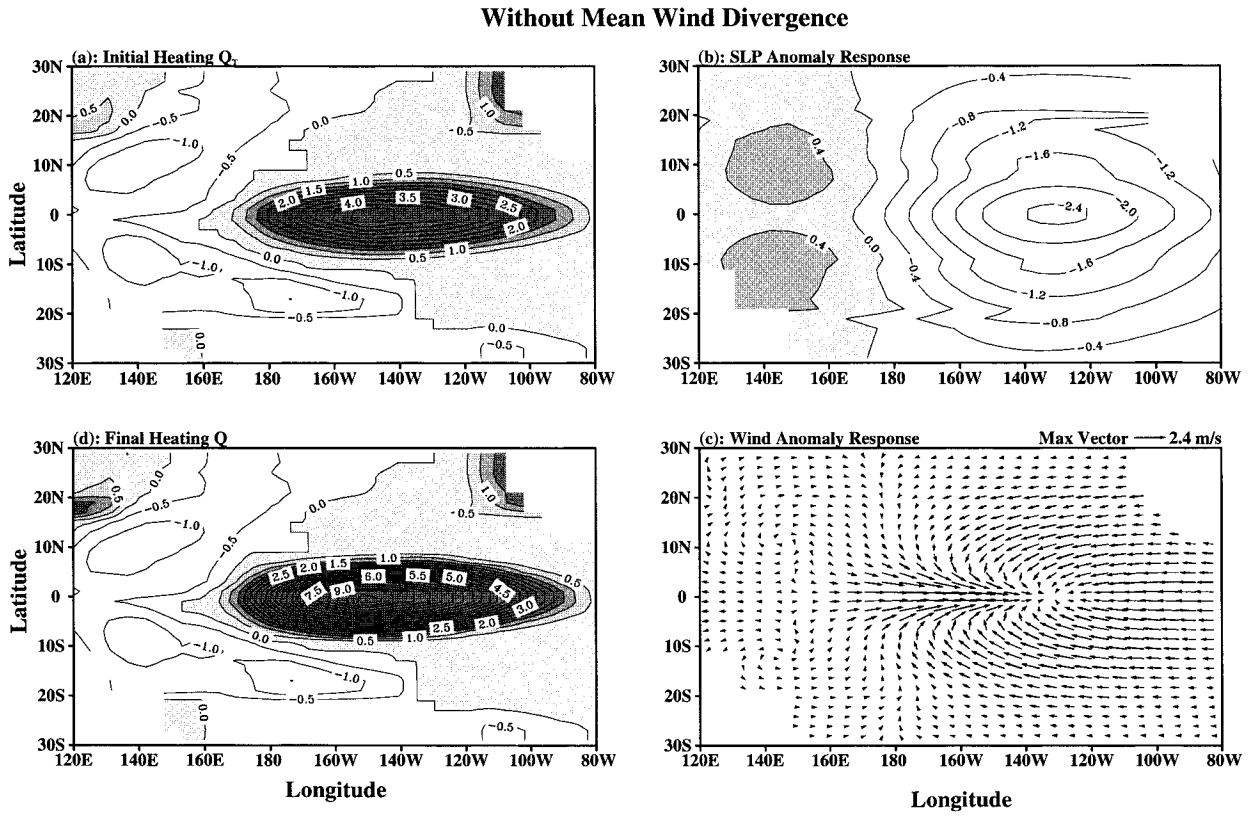

FIG. 6. As in Fig. 4, but without the mean wind divergence field.

the model with the off-equatorial western Pacific cold SST anomalies removed (equivalent to removing off-equatorial western Pacific negative heating anomalies). The model responses are shown in Fig. 8. SLP anomalies in the eastern Pacific show similar responses to the experiment in Fig. 4. However, SLP anomalies in the western Pacific do not show off-equatorial high SLP responses. Correspondingly, there are no equatorial easterly wind anomalies in the western Pacific. A comparison between Figs. 4 and 8 shows that although SLP anomaly response patterns in the eastern Pacific are similar, the westerly wind anomaly responses in the equatorial central Pacific for the experiment without off-equatorial patterns are smaller. This is because off-equatorial cold SST anomalies in the western Pacific also contribute to westerly wind anomalies in the equatorial central Pacific. Wang et al. (1999b) have shown that a pair of symmetric, off-equatorial cold SST anomalies in the western Pacific produces a pair of symmetric off-equatorial western Pacific high SLP anomalies, resulting in SLP patterns of relatively high and low SLP anomalies in the western and eastern Pacific, respectively. This SLP distribution produces equatorial easterly wind anomalies over the western Pacific and equatorial westerly wind anomalies to the east of the off-equatorial cold SST anomalies. Contributions to the equatorial westerly wind anomalies in the central Pacific are made by both positive heating anomalies in the equatorial central/eastern Pacific and negative heating anomalies in the off-equatorial western Pacific. Removing the off-equatorial negative heating anomalies in the western Pacific reduces the equatorial westerly wind anomalies in the central Pacific.

From this experiment, it can be concluded that the equatorial easterly wind anomalies in the western Pacific observed during the mature phase of El Niño can be produced by off-equatorial western Pacific cold SST anomalies, and that parts of the equatorial westerly wind anomalies in the central Pacific during the mature phase of El Niño are also produced by the off-equatorial western Pacific cold SST anomalies. Although these off-equatorial cold SST anomalies are smaller than warm SST anomalies in the equatorial eastern Pacific, they are sufficient to produce equatorial easterly wind anomalies in the western Pacific and equatorial westerly wind anomalies in the central Pacific, owing to the atmospheric mean background state. In the Gill–Zebiak model, atmospheric mean convergence associated with the convection of the western Pacific warm pool favors western Pacific anomaly growth.

e. Case without moisture convergence feedback process

Section 3c shows that the mean wind divergence field in the low-level moisture feedback process plays an im-

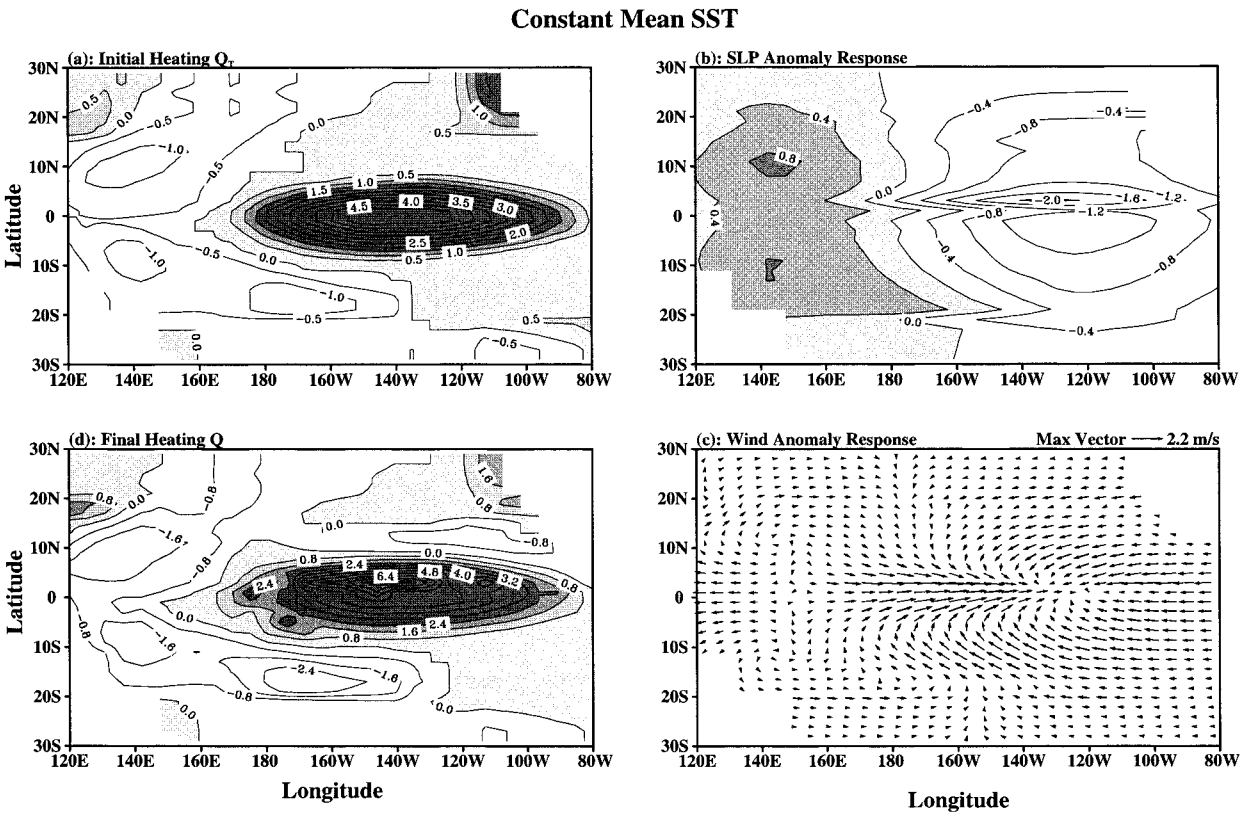

FIG. 7. As in Fig. 4, but with a constant mean SST ($\overline{T}$ = 27°C).

portant role in producing tropical atmospheric responses. The question is, what will happen if the low-level moisture convergence feedback process is excluded from the Gill–Zebiak model? In other words, will the pure Gill atmospheric model with modified heating, which depends upon mean and anomalous SST, produce realistic atmospheric responses? Figure 9 shows the model results for a case without the moisture convergence feedback ($\beta = 0$). The basic patterns of tropical atmospheric responses remain the same as experiments with the moisture convergence feedback. The atmospheric responses show low SLP anomalies in the eastern Pacific and off-equatorial high SLP anomalies in the western Pacific. Correspondingly, surface wind responses show equatorial westerly anomalies in the central Pacific and equatorial easterly wind anomalies in the western Pacific. However, the amplitudes of these responses are smaller than those for the case with the low-level moisture convergence feedback shown in Fig. 4. The low-level moisture convergence feedback amplifies atmospheric responses (Zebiak 1982, 1986). Without this feedback, SLP and wind anomaly responses show smaller values than observations.

f. Seasonal dependence

The atmospheric mean wind divergence varies seasonally, owing to the seasonal north–south migrations of the ITCZ and the South Pacific convergence zone (SPCZ). Figure 10 shows the mean wind divergence fields in March, June, September, and December specified in the Gill–Zebiak model, based on the mean wind observations of Rasmusson and Carpenter (1982). The ITCZ is southernmost (northernmost) to the equator and weaker (stronger) in the boreal spring (fall), whereas the SPCZ is northernmost (southernmost) to the equator and weaker (stronger) in the boreal fall (spring). The southernmost and northernmost locations of the ITCZ cause negative and positive divergence values in the equatorial eastern Pacific, respectively. Since the mean wind divergence field plays an important role in the Gill–Zebiak model, the seasonal variations in the mean wind divergence must affect the model atmospheric responses.

Two more experiments were performed with the model December climatologies replaced by the March and September climatologies. The model results are shown in Figs. 11 and 12. The atmospheric responses show stronger SLP and wind anomalies in the equatorial eastern Pacific during the boreal spring than during the boreal fall. This is because the equatorial eastern Pacific shows the mean wind convergence and divergence during the boreal spring and fall, respectively, associated with the seasonal movement of the ITCZ. According to Eq. (2), the mean wind convergence in the equatorial

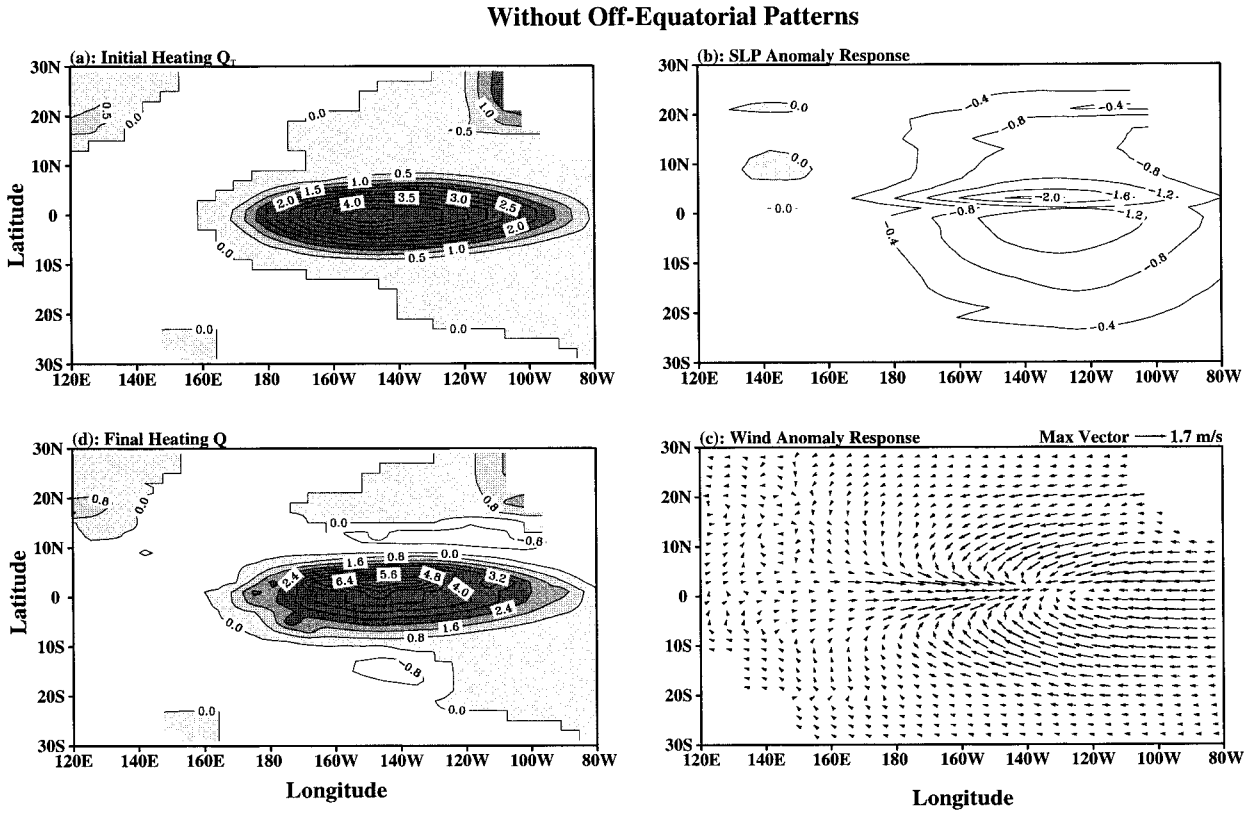

FIG. 8. As in Fig. 4, but without the off-equatorial western Pacific cold SST anomalies.

eastern Pacific during the boreal spring results in $Q_C = -\beta C$, whereas the mean wind divergence during the boreal fall induces $Q_C = 0$. Therefore, Q_C adds additional heating to initial heating in the equatorial eastern Pacific during the boreal spring, but it does not change initial heating during the boreal fall. The greater atmospheric heating during the boreal spring causes stronger low SLP anomalies in the equatorial eastern Pacific and stronger westerly wind anomalies in the equatorial central Pacific.

The seasonal dependence of atmospheric responses may provide a possible explanation for the ENSO phase-locking to the seasonal cycle. During the boreal spring, when the ITCZ is closer to the equator, there is a convergence of mean winds and this mean convergence enhances atmospheric heating due to the moisture convergence feedback. Enhancing atmospheric heating increases the westerly wind anomalies, which, in turn, affect SST anomalies through changing the thermocline and ocean circulation. Therefore, the equatorward movements of the ITCZ during boreal spring creates a positive feedback, that is, a coupled ocean–atmosphere instability. The instability favors perturbations to grow during that time. The boreal spring season, therefore, is a season during which the onset phase of El Niño is favorable to occur (Philander 1983; Hirst 1986). The converse occurs during the boreal fall. The northmost location of the ITCZ during the boreal fall causes a weak coupled instability that does not favor anomaly growth. When El Niño reaches its peak phase, the time derivative of SST anomalies vanishes. This occurs when the warming trend terms in the SST equations balance the cooling trend terms. Since it takes time for the coupled system to adjust to this balance, the peak warming may occur a few months later. Therefore, the SST anomalies in the equatorial eastern Pacific peak in the boreal late fall or in the boreal early winter.

4. Summary and discussion

The horizontal structure of the atmospheric heating anomalies in the tropical Pacific during the mature phase of El Niño is observed to differ from that of the SST anomalies. The spatial pattern differences include 1) the atmospheric heating anomalies being confined closer to the equator than the SST anomalies, and 2) maxima of positive and negative heating anomalies being located farther west than the SST anomalies. However, the Gill–Zebiak model assumes that the atmospheric initial heating has the same spatial patterns as the SST anomalies. This assumption is a cause of the model simulation deficiencies. When the model atmospheric heating is modified to resemble the anomaly fields manifesting the atmospheric heating, most of the model deficiencies have

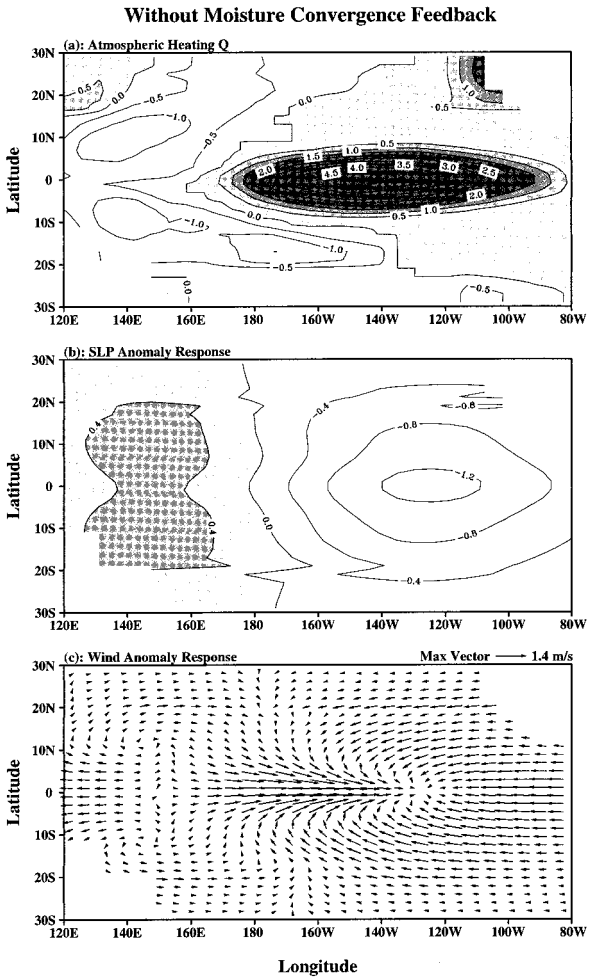

FIG. 9. Atmospheric reponses without the low-level moisture convergence feedback ($\beta = 0$). (a) Atmospheric heating $Q = Q_T$ (10^{-2} m^2 s^{-3}), (b) SLP anomaly response (mb), (c) surface wind anomaly response (m s^{-1}).

been eliminated. In particular, equatorial easterly wind anomalies in the western Pacific observed during the mature phase of El Niño are simulated very well. The region of maximum simulated equatorial westerly wind anomalies is shifted to the central Pacific, which is more consistent with observations. Unrealistic easterly wind anomalies produced in the off-equatorial eastern Pacific are reduced.

These improvements in the atmospheric model simulation may have implications in simulating ENSO by a coupled ocean–atmosphere model. Equatorial easterly wind anomalies in the western Pacific during the mature phase of El Niño provide an additional negative feedback for the coupled system (Weisberg and Wang 1997; Wang et al. 1999b; Wang 2000), by forcing upwelling Kelvin waves that propagate eastward and then affect anomalies in the equatorial eastern Pacific (Tang and Weisberg 1984; Philander 1985). This negative feedback induced by equatorial easterly wind anomalies in the western Pacific and the negative feedback of the delayed oscillator produced by wave reflection at the western boundary are both important in affecting the evolution of ENSO (Wang 2000). Thus, a better simulation of equatorial easterly wind anomalies in the western Pacific may help improve simulations of ENSO in coupled models. In addition, correctly simulating the position of maximum westerly wind anomalies may improve simulations of the position of warm SST anomalies, since wind and SST anomaly patterns closely follow each other (Zebiak and Cane 1987). Moreover, realistically simulating off-equatorial wind anomalies in the eastern Pacific will also help to simulate thermocline anomalies in the off-equatorial western Pacific, since the off-equatorial western Pacific thermocline variations are controlled by both local wind stress curl and the zonally integrated effect of off-equatorial Rossby waves (e.g., Meyers 1979; Kessler 1990).

Previous studies have used different heating anomalies to study tropical atmospheric responses by Gill-type model. For example, Gill and Rasmusson (1983) first used the horizontal pattern of the OLR anomalies from the 1982–83 ENSO event as a proxy for heating anomalies. Nigam and Shen (1993) performed rotated principal component analysis on OLR data and then used the leading mode of their principal analysis to force the Gill–Zebiak model. Dewitte and Perigaud (1996) parameterized heating anomalies in terms of the product of the first EOF mode horizontal structure of the cloud convection data and the Niño-3 SST anomalies, with the horizontal structure pattern of heating independent of time. The OLR-related heating parameterizations may be not applicable to the Zebiak and Cane coupled model since the coupled model does not calculate OLR anomalies. The Dewitte and Perigaud parameterization is applicable, but it is unrealistic since the horizontal pattern of heating anomalies is independent of time. It is not easy to parameterize heating anomalies correctly in terms of SST anomalies in a coupled ocean–atmosphere model. One method is to modify heating anomalies from SST anomalies, as suggested in this paper. However, since SST anomaly patterns in a coupled model are changed in every coupled step, the reconstructed function $A(T)$ should also be changed. In coupled ocean–atmosphere models, the reconstructed function must be designed to manifest pattern variations with time. In nature, the atmospheric convection is not necessarily related to SST anomalies. Graham and Barnett (1987) showed that the SST must be at least 28°C before deep convection occurs. Deep convection does not occur in the equatorial eastern Pacific, despite the large SST anomalies there, because the total water temperature is too low. This condition should also be considered in model heating parameterizations.

Kleeman (1991) forced the Gill-type model using atmospheric heating that differs from that of Zebiak (1986). He assumed that the latent heating results from changes in deep convective precipitation. Precipitation

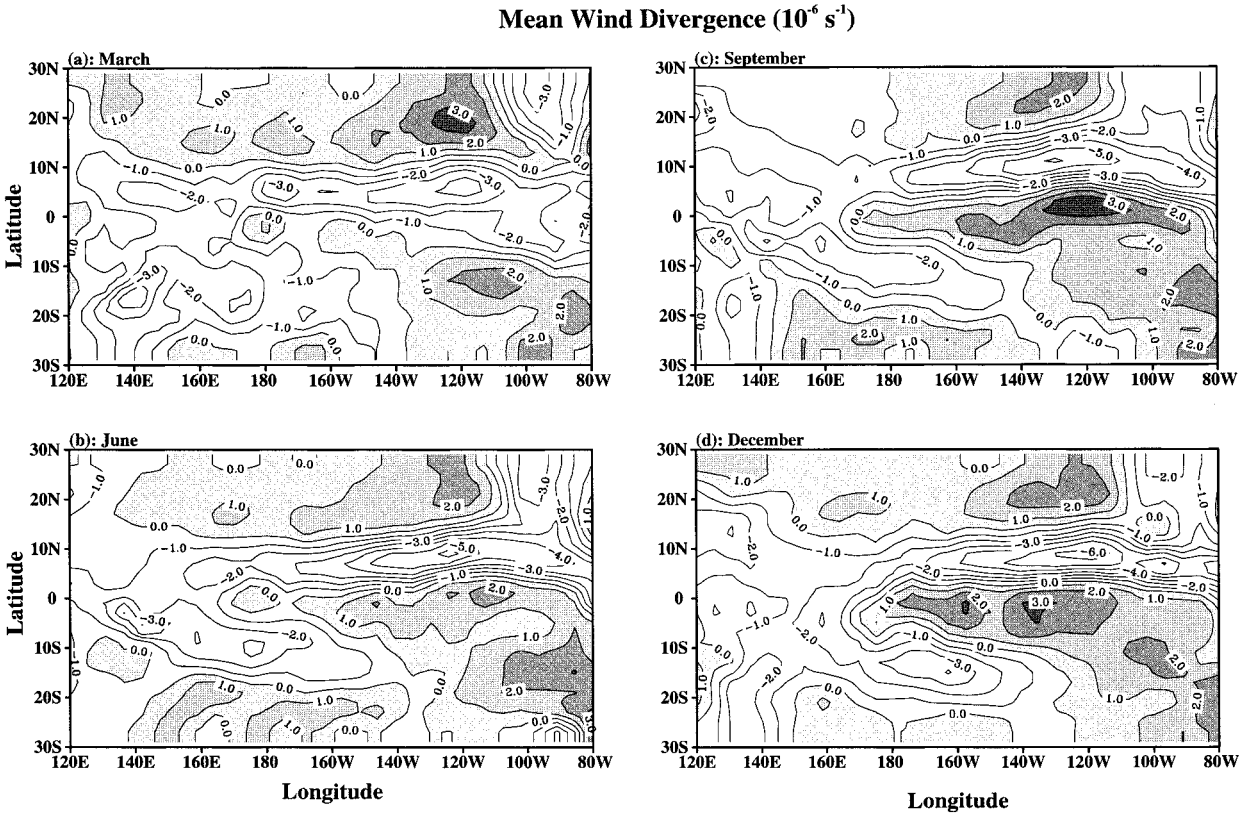

FIG. 10. The mean wind divergence field (10^{-6} s^{-1}) in (a) Mar, (b) Jun, (c) Sep, and (d) Dec specified in the Gill–Zebiak model.

changes are calculated from the vertically integrated steady state moisture equation perturbing about climatologies. In his model, precipitation is only allowed when the total SST is above a critical value (e.g., 28°C). In comparison with the Gill–Zebiak model, the model produces more realistic wind anomalies in the eastern Pacific (see his Figs. 3a and 13a). This is attributed to the fact that the model confines the heating to high total SST regions, which produces more realistic atmospheric heating than the Gill–Zebiak model does. The result of Kleeman (1991) is consistent with the result herein, supporting that the assumption of the heating parameterization in the Gill–Zebiak model is a cause of the model simulation deficiencies.

Battisti et al. (1999) summarized the two popular simple atmospheric models of Gill (1980) and Lindzen and Nigam (1987) and pointed out some inconsistencies between model derivation and the values of several of the parameters that required for these models to achieve reasonable circulation, rather than focus on model simulation deficiencies of these models. The Gill (or Gill–Zebiak) model needs an extremely short damping time (1–2 days) to horizontally confine the response and produce reasonable meridional wind anomalies. The model also needs flux anomalies, averaged over a typical ENSO event, to be four to five times larger than those observed (surface heating anomalies from evaporation are observed in a range of 15–20 W m^{-2} for a 1°C temperature anomaly, whereas the model is in excess of 75 W m^{-2}). The Lindzen and Nigam model assumes that surface convergence associated with convection is everywhere, whereas there are large regions of the Tropics that rarely experience deep convection in nature. The Lindzen and Nigam model requires an unjustifiably short thermal damping time to achieve physically reasonable solution.

Recognizing the problems of the Lindzen and Nigam model, Battisti et al. (1999) developed a new model of the reduced gravity atmospheric model that is similar to the Lindzen and Nigam model. The difference is that the rate of relaxation of the boundary layer perturbations in the reduced gravity model depends on whether or not there is enough moisture to support convection. They assumed that when convection is diagnosed, the venting of the boundary layer is taken as the timescale associated with the life cycle of deep convection. In the absence of deep convection, the mixing out of the boundary layer perturbations is at slower entrainment rate in order of 1–2 days. Although the physics of the Gill–Zebiak model, the Lindzen and Nigam model, and the reduced gravity model are different, numerical solutions of atmospheric responses to a specified SST anomaly pattern are similar (not shown). In fact, Battisti et al. (1999) showed that the mathematical formulation

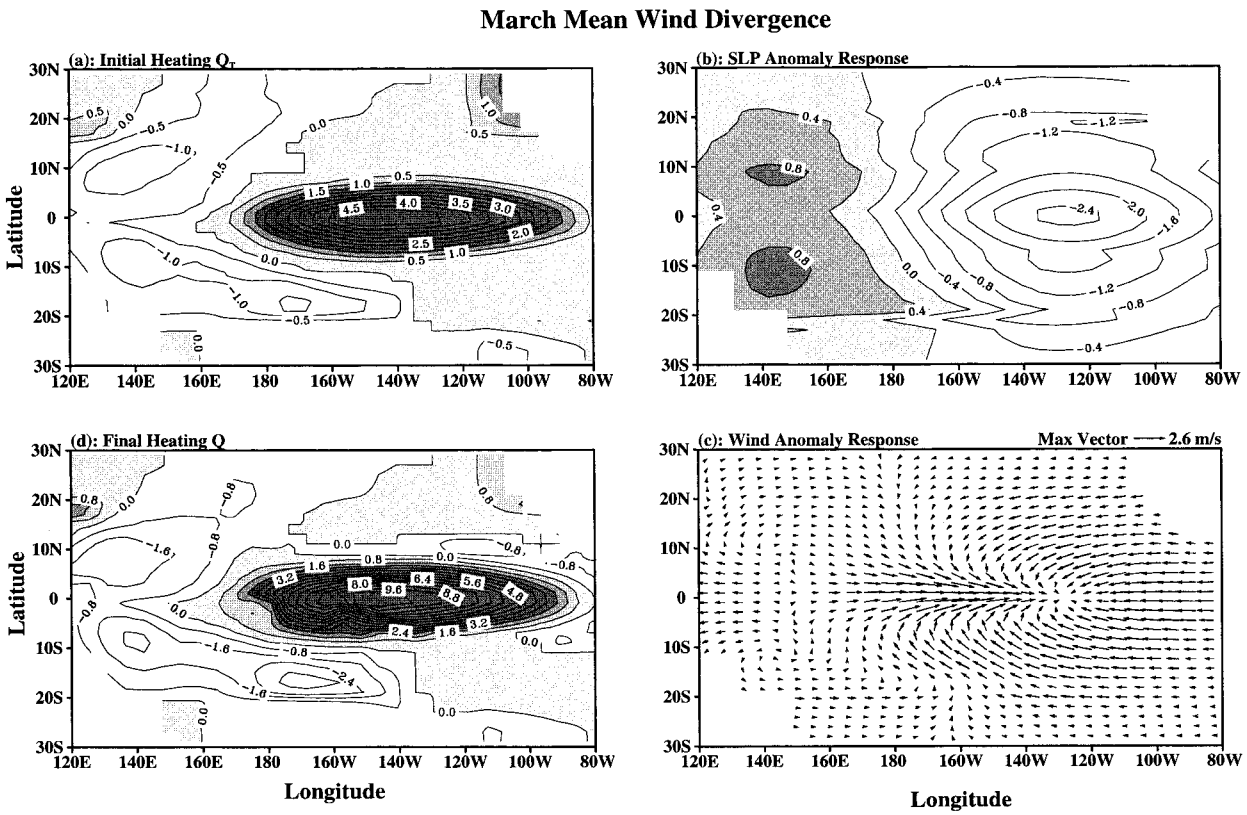

FIG. 11. As in Fig. 4, but with the model Dec climatologies replaced by the Mar climatologies.

of the reduced gravity model is identical to the Gill–Zebiak model. Neelin (1989) also noted the mathematical similarity of the Gill model to the Lindzen and Nigam model, although the physics is fundamentally different. Therefore, the conclusions regarding the Gill–Zebiak model are also held in the Lindzen and Nigam model and the reduced gravity model.

In the Gill–Zebiak model, there are two mean background states. Among these two mean background states, the mean wind divergence field plays a relatively more important role than the mean SST for determining atmospheric responses. This is consistent with the recent analyses of Tziperman et al. (1997), who showed that the mean wind divergence is the most important background state in the coupled ocean–atmosphere model of Zebiak and Cane (1987). The mean wind divergence is incorporated into the Gill–Zebiak model through the parameterization of the low-level moisture convergence feedback process. Although this feedback may be oversimplified for considering atmospheric moisture effects, it has significantly improved the model results (Zebiak 1986). The mean wind divergence field in this feedback process plays a key role for the model to simulate equatorial easterly wind anomalies in the western Pacific during the mature phase of El Niño. The mean atmospheric state in the western Pacific is convergent, induced by the atmospheric convection associated with the western Pacific warm pool waters. The mean wind convergence favors anomaly growth in the western Pacific. Without the mean wind divergence field, the model fails to produce equatorial easterly wind anomalies in the western Pacific.

Model ENSO phase-locking to the seasonal cycle has been previously hypothesized to be due to the interactions between the annual forcing and interannual oscillations (e.g., Jin et al. 1994; Tziperman et al. 1994; Chang et al. 1995; Wang et al. 1999a). Recently, Wang and Fang (1996) and Tziperman et al. (1998) argued that the seasonal dependence of coupled ocean–atmosphere instability may be responsible for the ENSO phase-locking. Both of these theories depend upon the seasonal cycle in the coupled system. The model results herein seem to support the latter theory. The seasonal north–south migrations of the ITCZ cause seasonal variations of the mean wind divergence field in the equatorial eastern Pacific. The mean wind divergence field induces the strongest and weakest instability in the boreal spring and fall, respectively. When the ocean–atmosphere system adjusts to a state in which the warming trends balance the cooling trends in the SST equation, El Niño reaches its peak. This may explain why the SST anomalies in the equatorial central and eastern Pacific peak in the late fall or in the early winter. However, this cannot explain the phase-locking in the far eastern Pa-

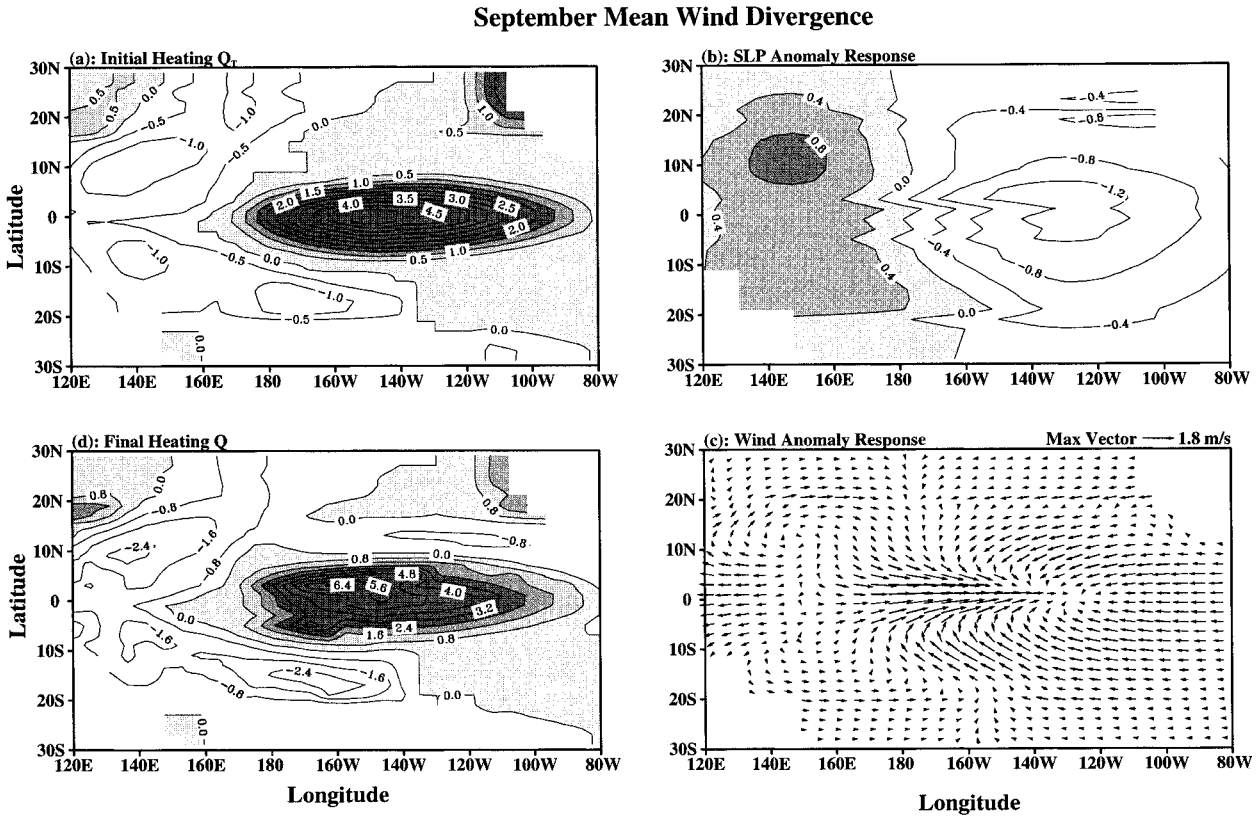

FIG. 12. As in Fig. 4, but with the model Dec climatologies replaced by the Sep climatologies.

cific, suggesting that the physics of the ENSO phase-locking in the far eastern Pacific is different (Wang et al. 1999a).

In summary, the paper investigates the atmospheric responses to tropical Pacific heating using the Gill–Zebiak model. The observed spatial structure of heating anomalies differs from that of the SST anomalies. The assumption of the same spatial structure between the heating and SST anomalies in the Gill–Zebiak model is a cause of model deficiencies in ENSO simulation. When the model heating forcing is modified to resemble the observed heating anomalies during the mature phase of El Niño, the simulations are improved. The improvements include the ability to 1) successfully simulate equatorial easterly wind anomalies in the western Pacific, 2) correctly simulate the position of maximum westerly wind anomalies, and 3) reduce unrealistic easterly wind anomalies in the off-equatorial eastern Pacific. This paper shows that the mean wind divergence field is an important background state, whereas the mean SST is secondary. Although off-equatorial cold SST anomalies in the western Pacific during the mature phase of El Niño are smaller than equatorial positive SST anomalies in the eastern Pacific, they are enough to produce atmospheric responses of comparable magnitude to the equatorial eastern Pacific. The cause of this relates to the atmospheric mean state being convergent in the western Pacific and divergent in the equatorial eastern Pacific. By removing the atmospheric mean divergence field, the model fails to produce equatorial easterly wind anomalies observed in the western Pacific during the mature phase of El Niño. If off-equatorial cold SST anomalies in the western Pacific are removed, the atmospheric responses show no equatorial easterly wind anomalies in the western Pacific and a decrease in equatorial westerly wind anomalies in the central Pacific during the mature phase of El Niño.

Acknowledgments. This work was supported by the NASA Seasonal-to-Interannual Prediction Project (NSIPP). Discussions with D. Enfield, D. Mayer, R. Weisberg, and J. Virmani are appreciated. I thank S. Zebiak for providing his model code.

REFERENCES

Battisti, D. S., E. S. Sarachik, and A. C. Hirst, 1999: A consistent model for the large-scale steady surface atmospheric circulation in the Tropics. *J. Climate*, **12,** 2956–2964.

Bjerknes, J., 1966: A possible response of the atmospheric Hadley circulation to equatorial anomalies of ocean temperature. *Tellus*, **18,** 820–829.

——, 1969: Atmospheric teleconnections from the equatorial Pacific. *Mon. Wea. Rev.*, **97,** 163–172.

Chang, P., L. Ji, B. Wang, and T. Li, 1995: Interactions between the

seasonal cycle and El Niño–Southern Oscillation in an intermediate coupled ocean–atmosphere model. *J. Atmos. Sci.,* **52,** 2353–2372.
Chao, Y., and S. G. H. Philander, 1993: On the structure of the southern oscillation. *J. Climate,* **6,** 450–469.
Deser, C., and J. M. Wallace, 1990: Large-scale atmospheric circulation features of warm and cold episodes in the tropical Pacific. *J. Climate,* **3,** 1254–1281.
Dewitte, B., and C. Perigaud, 1996: El Niño–La Niña events simulated with Cane and Zebiak's model and observed with satellite or in situ data. Part II: Model forced with observations. *J. Climate,* **9,** 1188–1207.
Gill, A. E., 1980: Some simple solutions for heat-induced tropical circulation. *Quart. J. Roy. Meteor. Soc.,* **106,** 447–462.
——, and E. M. Rasmusson, 1983: The 1982–83 climate anomaly in the equatorial Pacific. *Nature,* **306,** 229–234.
Graham, N. E., and T. P. Barnett, 1987: Sea surface temperature, surface wind divergence, and convection over tropical oceans. *Science,* **238,** 657–659.
——, and W. B. White, 1988: The El Niño cycle: A natural oscillator of the Pacific Ocean–atmosphere system. *Science,* **240,** 1293–1302.
——, and ——, 1991: Comments on ''On the role of off-equatorial oceanic Rossby waves during ENSO.'' *J. Phys. Oceanogr.,* **21,** 453–460.
Hirst, A. C., 1986: Unstable and damped equatorial modes in simple coupled ocean–atmosphere models. *J. Atmos. Sci.,* **43,** 606–630.
Jin, F.-F., J. D. Neelin, and M. Ghil, 1994: El Niño on the devil's staircase: Annual subharmonic steps to chaos. *Science,* **264,** 70–72.
Kessler, W. S., 1990: Observations of long Rossby waves in the northern tropical Pacific. *J. Geophys. Res.,* **95,** 5183–5219.
Kleeman, R., 1991: A simple model of the atmospheric response to ENSO sea surface temperature anomalies. *J. Atmos. Sci.,* **48,** 3–18.
Latif, M., J. Biercamp, H. von Storch, M. J. McPhaden, and E. Kirk, 1990: Simulation of ENSO-related surface wind anomalies with an atmospheric GCM forced by observed SST. *J. Climate,* **3,** 509–521.
Lindzen, R. S., and S. Nigam, 1987: On the role of sea surface temperature gradients in forcing low-level winds and convergence in the tropics. *J. Atmos. Sci.,* **44,** 2418–2436.
McCreary, J. P., and D. L. T. Anderson, 1991: An overview of coupled ocean-atmosphere models of El Niño and the Southern Oscillation. *J. Geophys. Res.,* **96,** 3125–3150.
Mestas-Nunez, A. M., and D. B. Enfield, 2000: Eastern equatorial Pacific SST variability: ENSO and non-ENSO components and their climatic associations. *J. Climate,* in press.
Meyers, G., 1979: On the annual Rossby wave in the tropical north Pacific Ocean. *J. Phys. Oceanogr.,* **9,** 663–674.
Mitchell, T. P., and J. M. Wallace, 1996: ENSO seasonality: 1950–78 versus 1979–92. *J. Climate,* **9,** 3149–3161.
Neelin, J. D., 1989: On the interpretation of the Gill model. *J. Atmos. Sci.,* **46,** 2466–2468.
——, D. S. Battisti, A. C. Hirst, F.-F. Jin, Y. Wakata, T. Yamagata, and S. E. Zebiak, 1998: ENSO theory. *J. Geophys. Res.,* **103,** 14 262–14 290.
Nigam, S., and H. S. Shen, 1993: Structure of oceanic and atmospheric low-frequuency variability over the tropical Pacific and Indian Oceans. Part I: COADS observations. *J. Climate,* **6,** 657–676.
Philander, S. G., 1983: El Niño Southern Oscillation phenomena. *Nature,* **302,** 295–301.
——, 1985: El Niño and La Niña. *J. Atmos. Sci.,* **42,** 2652–2662.
——, 1990: *El Niño, La Niña, and the Southern Oscillation.* Academic Press, 289 pp.
Rasmusson, E. M., and T. H. Carpenter, 1982: Variations in tropical sea surface temperature and surface wind fields associated with the Southern Oscillation/El Niño. *Mon. Wea. Rev.,* **110,** 354–384.
——, and J. M. Wallace, 1983: Meteorological aspects of the El Niño/Southern Oscillation. *Science,* **222,** 1195–1202.
Seager, R., and S. E. Zebiak, 1995: Simulation of tropical climate with a linear primitive equation model. *J. Climate,* **8,** 2497–2520.
Tang, T. Y., and R. H. Weisberg, 1984: On the equatorial Pacific response to the 1982/1983 El Niño-Southern Oscillation event. *J. Mar. Res.,* **42,** 809–829.
Tziperman, E., L. Stone, M. Cane, and H. Jarosh, 1994: El Niño chaos: Overlapping of resonances between the seasonal cycle and the Pacific ocean-atmosphere oscillator. *Science,* **264,** 72–74.
——, S. E. Zebiak, and M. A. Cane, 1997: Mechanisms of seasonal–ENSO interaction. *J. Atmos. Sci.,* **54,** 61–71.
——, M. A. Cane, S. E. Zebiak, Y. Xue, and B. Blumenthal, 1998: Locking of El Niño's peak time to the end of the calender year in the delayed oscillator picture of ENSO. *J. Climate,* **11,** 2191–2199.
Wang, B., and T. Li, 1993: A simple tropical atmosphere model of relevance to short-term climate variations. *J. Atmos. Sci.,* **50,** 260–284.
——, and Z. Fang, 1996: Chaotic oscillation of tropical climate: A dynamical system theory for ENSO. *J. Atmos. Sci.,* **53,** 2786–2802.
Wang, C., 2000: A unified oscillator model for the El Niño–Southern Oscillation. *J. Climate,* in press.
——, and R. H. Weisberg, 2000: The 1997–98 El Niño evolution relative to previous El Niño events. *J. Climate,* **13,** 488–501.
——, ——, and H. Yang, 1999a: Effects of the wind speed–evaporation–SST feedback on the El Niño–Southern Oscillation. *J. Atmos. Sci.,* **56,** 1391–1403.
——, ——, and J. I. Virmani, 1999b: Western Pacific interannual variability associated with the El Niño-Southern Oscillation. *J. Geophys. Res.,* **104,** 5131–5149.
Webster, P. S., 1981: Mechanisms determining the atmospheric response to sea surface temperature anomalies. *J. Atmos. Sci.,* **38,** 554–571.
Weisberg, R. H., and C. Wang, 1997: A western Pacific oscillator paradigm for the El Niño–Southern Oscillation. *Geophys. Res. Lett.,* **24,** 779–782.
White, W. B., S. E. Pazan, and M. Inoue, 1987: Hindcast/forecast of ENSO events based on redistribution of observed and model heat content in the western tropical Pacific, 1964–1986. *J. Phys. Oceanogr.,* **17,** 264–280.
——, Y. H. He, and S. E. Pazan, 1989: Off-equatorial westward propagating Rossby waves in the tropical Pacific during the 1982–83 and 1986–87 ENSO events. *J. Phys. Oceanogr.,* **19,** 1397–1406.
Woodruff, S. D., R. J. Slutz, R. L. Jenne, and P. M. Steurer, 1987: A comprehensive ocean–atmosphere data set. *Bull. Amer. Meteor. Soc.,* **68,** 1239–1250.
Zebiak, S. E., 1982: A simple atmospheric model of relevance to El Niño. *J. Atmos. Sci.,* **39,** 2017–2027.
——, 1985: Tropical atmosphere-ocean interaction and the El Niño-Southern Oscillation phenomenon. Ph.D. thesis, Massachusetts Institute of Technology, 261 pp.
——, 1986: Atmospheric convergence feedback in a simple model for El Niño. *Mon. Wea. Rev.,* **114,** 1263–1271.
——, 1990: Diagnostic studies of Pacific surface winds. *J. Climate,* **3,** 1016–1031.
——, and M. A. Cane, 1987: A model El Niño–Southern Oscillation. *Mon. Wea. Rev.,* **115,** 2262–2278.